

# Validation of an entropy-viscosity model for large eddy simulation

J.-L. Guermond, A. Larios, and T. Thompson

## 1 Introduction

A primary mainstay of difficulty when working with problems of very high Reynolds numbers is the lack of computational resources; this implies that numerical simulations in this realm are, in general, always under-resolved. That is, large gradients and eddy-phenomena, exist at the sub-grid level and cannot be correctly represented by the mesh; therefore, at the mesh scale, these solutions can be considered as behaving in a singular manner. As time progresses, these unresolved facets of the flow are likely to produce still larger gradients through the coupling of wave modes via the action of the nonlinear term; this induces an accumulation of energy at the grid scale. A solution proposed in [GPP11b] consists of monitoring the local kinetic energy balance and introducing a localized dissipation in these regions that is proportional to the violation of this balance (this is the so-called entropy viscosity). The deviation from the local energy balance (which we call the entropy residual) can be thought of as an indicator for local entropy production in analogy with entropy production for scalar conservation laws.

### 1.1 Motivation

Here a brief overview of the motivation for the entropy-viscosity is presented. See [GPP11b] and the references therein for a more in-depth discussion of the central ideas of the entropy-viscosity technique.

Let  $(u_h, p_h)$  be an approximate velocity and pressure, where  $h$  denotes the grid scale, and define the numerical residual of the energy equation,  $D_h(x, t)$ , by

---

Department of Mathematics, Texas A&M University, College Station, TX 77843, USA  
e-mail: [guermond@math.tamu.edu](mailto:guermond@math.tamu.edu), [alarios@math.tamu.edu](mailto:alarios@math.tamu.edu), [tthompson@tennessee.edu](mailto:tthompson@tennessee.edu)

$$D_h(x, t) := \partial_t \left( \frac{1}{2} u_h^2 \right) + \nabla \cdot \left( \left( \frac{1}{2} u_h^2 + p_h \right) u_h \right) - Re^{-1} \Delta \left( \frac{1}{2} u_h^2 \right) + Re^{-1} (\nabla u_h)^2 - f \cdot u_h. \quad (1)$$

In a resolved flow  $D_h(x, t)$  should be on the order of the consistency error of the method; a large value<sup>1</sup> of  $|D_h(x, t)|$  is caused by under-resolution. In such situations, one would therefore wish to enforce

$$|D_h(x, t)| = 0. \quad (2)$$

However, enforcing (2) directly may over-determine the problem. In [GPP11b], the authors circumvent this difficulty by constructing a viscosity proportional to  $|D_h(x, t)|$ . This viscosity is called the entropy-viscosity (EV), and is defined by

$$\nu_E(x, t) := \min \left( c_{max} h(x) |u_h(x, t)|, c_E h^2(x) \frac{|D_h(x, t)|}{\|u^2\|_{L^\infty(\Omega)}} \right). \quad (3)$$

The momentum equation is then modified by adding the term  $-\nabla \cdot (\nu_E(x, t) \nabla u)$ . The entropy-viscosity<sup>2</sup> regularizes regions which are in violation of (2) and promotes a dissipative effect on numerical singularities.

In definition (3), the constants  $c_{max}$  and  $c_E$  are tunable parameters which depend only on the numerical method and the geometry of the mesh. For instance, in the setting of scalar conservation laws, the analogue of (3) gives  $c_{max} = \frac{1}{2}$  in one space dimension with piecewise linear finite elements. Definition (3) ensures that the LES viscosity will never exceed the first-order upwind viscosity. When  $h(x)$ , the local grid size, is small enough so that all scales are resolved, then  $|D_h(x, t)|$  is on the order of the consistency error. Hence, the LES viscosity which is proportional to  $h^2(x) |D_h(x, t)|$ , is far smaller than the first order upwind viscosity. The entropy-viscosity is therefore consistent, and it vanishes when all of the scales of the flow are properly resolved at the grid scale. The remainder of this paper details the context in which the entropy viscosity was tested as well as the ensuing numerical results.

## 2 Numerical Method

Our investigations into the efficacy of the entropy-viscosity for regularizing the Navier-Stokes equation are carried out via a well-verified periodic spectral code discussed in the context of [TKE03] and [KTM04]. Entropy-viscosity in the setting of bounded domains, utilizing an ADI approach found in [GMS12], is currently being investigated by the authors; results will appear in a forthcoming paper. The spectral code mentioned above has been well validated [CDK<sup>+</sup>05, TKE03, KTM04]. Standard 2/3's de-aliasing was utilized in a periodic box of length  $L = 1$ . The time-stepping scheme implemented is a fully explicit four-stage Runge-Kutta method

<sup>1</sup> The sign of the residual has a physical interpretation discussed in [GPP11b].

<sup>2</sup> For a discussion of a generalized framework for definition an entropy-viscosity, presented in the context of hyperbolic conservation laws, see [GPP11a].

with dynamic time-stepping respecting the CFL condition. The entropy-viscosity is formed via the canonical pseudo-spectral technique whereby derivatives are computed in spectral space and products in physical space. For this situation,  $c_{max} = 0.1$  and  $c_E = 0.25$  were used in (3). The entropy-viscosity, computed explicitly following (3), is formulated using the current time step in conjunction with the two time-steps prior; BDF2 is employed to compute the time derivative. The result is applied, as a regularization, for the next time-step. The action of the entropy-viscosity is not present for the first three time-steps of the simulation; in practice this has caused no stability issues, even in the case of high Reynolds numbers. Finally, the divergence free condition is enforced exactly via projection onto the space of solenoidal vector fields. All the simulations presented here are done with a low-wave number forcing designed to keep the total kinetic energy approximately constant, as described in [OP98].

### 3 Results

In this section we discuss three main results: the consistency of the entropy-viscosity (i.e., when all scales are properly resolved, there is no noticeable contribution from the entropy-viscosity), energy spectrum verification results, and the action of the entropy-viscosity in the context of under-resolved and severely under-resolved flows. Results regarding additional statistics are forthcoming.

#### 3.1 Consistency

For a resolved flow, we expect that the contribution of the entropy-viscosity should be on the order of the local consistency error of the method. Indeed, the notion of entropy-viscosity is constructed to satisfy this requirement. It is expected that the entropy-viscosity should go to zero significantly faster than  $\mathcal{O}(h^2)$ .

We first test an inviscid flow with the following two-dimensional initial data:  $u = \cos(8\pi x)\sin(8\pi y)$ ,  $v = -\sin(8\pi x)\cos(8\pi y)$ ,  $w = 0$ . The flow remains two-dimensional at later times (i.e. laminar) and the total kinetic energy is constant in time. We compute the Euler solution up to  $t = 4$  using the DNS code, the entropy-viscosity technique and the Smagorinsky model on various grids ( $32^3$ ,  $64^3$ ,  $128^3$ ,  $256^3$ ). We show in Figure 1a the time evolution of the kinetic energy for the entropy-viscosity solution and the Smagorinsky solution on the  $32^3$  grid and that of the DNS solution on the  $256^3$  grid. It is striking that the Smagorinsky solution loses energy fast even though the flow is laminar, whereas the entropy-viscosity solution tracks the DNS solution rather closely. The reason why the entropy-viscosity model outperforms the Smagorinsky model is that the entropy-viscosity is very small since the flow is laminar. The entropy viscosity is significantly smaller than  $h^2$  due to the spectral accuracy of the Fourier approximation.

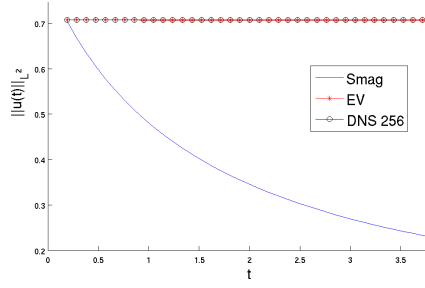


**Fig. 1a** Total energy vs. time for Smagorinsky and EV models for an inviscid flow at  $32^3$ .

	DNS	EV	Smag.
32	4.0e-13	2.1e-06	6.8e-1
64	1.6e-16	1.1e-06	3.6e-1
128	6.5e-14	5.6e-10	1.2e-1
256	1.1e-13	8.7e-11	3.3e-2

**Fig. 1b** Energy loss  $\|\mathbf{u} - \mathbf{u}_0\|_{L^2} / \|\mathbf{u}_0\|_{L^2}$  at  $t = 4$

We show in Figure 1b a table displaying the relative kinetic energy loss for the DNS, entropy-viscosity, and the Smagorinsky solutions at time  $t = 4$  on the four grids  $32^3$ ,  $64^3$ ,  $128^3$ ,  $256^3$ . We observe that the DNS does not lose any energy at all the resolutions and the entropy-viscosity solution does not lose any significant amount of energy, even at low resolution. The Smagorinsky solution on the other hand has lost 68% of the energy by time  $t = 4$  on the  $32^3$  grid and 3.3% on the  $256^3$  grid. This test confirms that contrary to the Smagorinsky method, the entropy-viscosity method does not dissipate energy in the laminar regions of the flow.

A full investigation of the consistency of the entropy viscosity method will be carried out in a forthcoming paper.

### 3.2 Entropy-Viscosity as an LES Model

We are interested in the applicability of the entropy-viscosity as an LES model. One expects that the entropy-viscosity should damp spurious high wave-mode contributions and resolve an otherwise unresolved flow. Therefore it is reasonable to conjecture that entropy-viscosity is well-suited to LES.

The fundamental question of whether or not the local energy balance, being enforced via the entropy-viscosity, evinces the quintessential dynamics of resolved flow, and to what extent, is addressed; specifically the Kolmogorov  $-\frac{5}{3}$  trend in the inertial range of the energy spectrum is examined.

We examine how entropy-viscosity effects the energy spectrum of under-resolved flows. In figures 2a–2d, we show the energy spectra of simulation runs at  $Re \approx 6500$  for various resolutions. All runs are compared against a resolved DNS run at resolution  $256^3$  (called “No Model”). Each under-resolved simulation is done using the entropy-viscosity model and the Smagorinsky model. One can see that unregularized (“No Model”) flows fail to capture the correct spectra as expected, while the flows regularized with entropy-viscosity perform significantly better. Note also that the entropy viscosity model is always closer to the DNS spectrum than the Smagorinsky model.

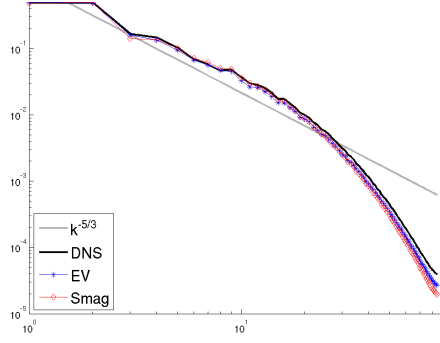


**Fig. 2a**  $256^3$  resolution with Entropy-Viscosity (EV) and with Smagorinsky (Smag). DNS simulation included for comparison (DNS).

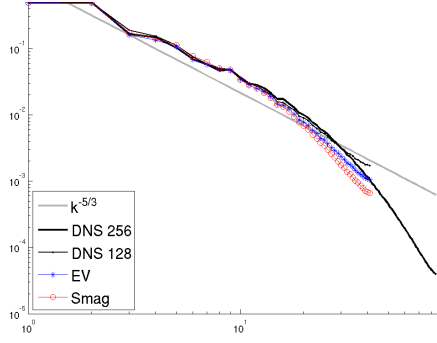


**Fig. 2b**  $128^3$  resolution: Entropy viscosity, unresolved DNS, Smagorinsky. “No Model”  $256^3$  DNS simulation included for comparison.

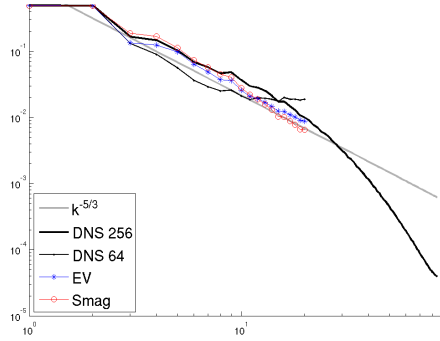


**Fig. 2c**  $64^3$  resolution: Entropy viscosity, unresolved DNS, Smagorinsky. “No Model”  $256^3$  DNS simulation included for comparison.

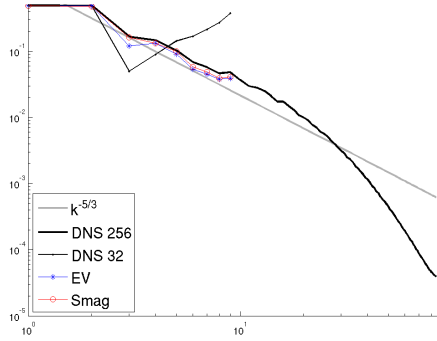


**Fig. 2d**  $32^3$  resolution: Entropy viscosity, unresolved DNS, Smagorinsky. “No Model”  $256^3$  DNS simulation included for comparison.

### 3.3 Structure of the Enstrophy

An important characteristic to capture in modeling isotropic turbulent flow is the structure of coherent vortex tubes, that is, the level sets of the enstrophy,  $|\nabla \times u(x, t)|$ . We compare vortex tubes of an unresolved simulation against a simulation with exactly the same parameters, except that entropy-viscosity is added. In figures **3a** and **3b**, several level-surfaces with values in a range of  $\approx 50\%$ - $75\%$  of the maximum enstrophy at the same fixed time step (taken after the flow has reached a statistical steady-state) are shown. While the enstrophy of the unresolved flow appears quite polluted (**Fig. 3a**), the enstrophy of the entropy-viscosity regularized flow (**Fig. 3b**) contains well-defined vortex tubes, and is more characteristic of turbulent flow.

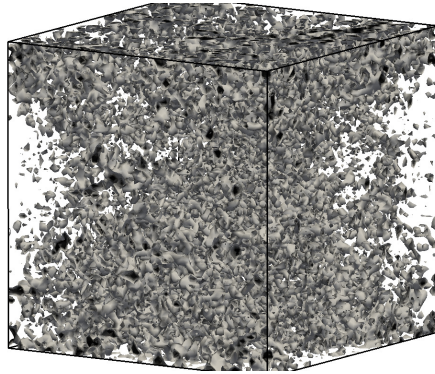


**Fig. 3a** Surfaces of constant enstrophy for a  $64^3$  simulation with  $Re \approx 6500$  (Unresolved). Darker surfaces indicate larger enstrophy.

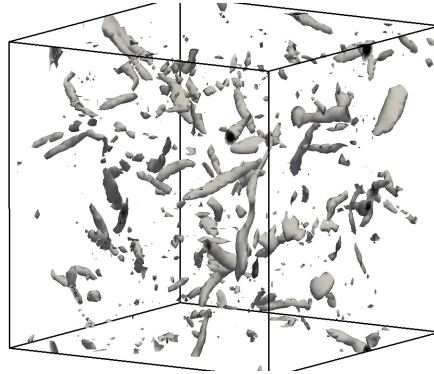


**Fig. 3b** Surfaces of constant enstrophy for a  $64^3$  simulation with  $Re \approx 6500$  with entropy-viscosity regularization at the same time step.

## References

- [CDK<sup>+</sup>05] S. Y. Chen, B. Dhruva, S. Kurien, K. R. Sreenivasan, and M. A. Taylor, *Anomalous scaling of low-order structure functions of turbulent velocity*, J. Fluid Mech. **533** (2005), 183–192. MR 2263308 (2007d:76141)
- [GMS12] Jean-Luc Guermond, Peter D. Mineev, and Abner J. Salgado, *Convergence analysis of a class of massively parallel direction splitting algorithms for the Navier-Stokes equations in simple domains*, Math. Comp. **81** (2012), no. 280, 1951–1977. MR 2945144
- [GPP11a] Jean-Luc Guermond, Richard Pasquetti, and Bojan Popov, *Entropy viscosity method for nonlinear conservation laws*, J. Comput. Phys. **230** (2011), no. 11, 4248–4267. MR 2787948 (2012h:65216)
- [GPP11b] ———, *From suitable weak solutions to entropy viscosity*, J. Sci. Comput. **49** (2011), no. 1, 35–50. MR 2831670
- [KTM04] Susan Kurien, Mark A. Taylor, and Takeshi Matsumoto, *Isotropic third-order statistic in turbulence with helicity: the 2/15-law*, J. Fluid Mech. **515** (2004), 87–97. MR 2260709
- [OP98] M.R. Overholt and S.B. Pope, *A deterministic forcing scheme for direct numerical simulations of turbulence*, Comput. Fluids **27** (1998), no. 1, 11–28.
- [TKE03] Mark A. Taylor, Susan Kurien, and Gregory L. Eyink, *Recovering isotropic statistics in turbulence simulations: the Kolmogorov 4/5th law*, Phys. Rev. E (3) **68** (2003), no. 2, 026310, 8. MR 2010083 (2004i:76126)